ELSEVIER

PII: S0032-3861(97)00571-5

Polymer Vol. 39 No. 12, pp. 2515–2520, 1998

0032-3861/98/$19.00+0.00

A birefringence study of polymer crystallization in the process of elongation of films

D. S. Ryu, T. Inoue* and K. Osaki
Institute for Chemical Research, Kyoto University, Uji, Kyoto 611, Japan
(Received 23 June 1997; accepted 9 July 1997)

The stress–birefringence relationship was examined for amorphous poly(ethylene terephthalate) films under uniaxial stretching in the temperature range 80–95°C at various stretch speeds in order to study the effect of strain-induced crystallization. At high temperatures, the ordinary stress–optical rule (SOR) held well at low draw ratios; the birefringence was proportional to the stress. However, at a certain draw ratio, the birefringence started to increase more rapidly than the stress and the SOR did not hold thereafter. D.s.c. measurements for films quenched at various stages of stretching supported the breakdown of the SOR being due to strain-induced crystallization. At still higher draw ratios, the stress suddenly began to increase. This is attributed to the non-Gaussian nature of the highly extended chains. The stress–optical coefficient has to be assumed to decrease with stress in order to estimate the crystallinity from the birefringence of films under high stress. At very low temperatures or at very high stretch speeds, the SOR was invalid even at low draw ratios due to the contribution of glassy stress. Even for such cases, the onset of strain-induced crystallization may be determined from the stress–birefringence relationship provided that the crystallization starts at relatively high draw ratios where the contribution from the glassy stress is small.

(Keywords: strain-induced crystallization; birefringence; stress–optical rule)

INTRODUCTION

The stress–birefringence relationship for deformed polymers has long been the subject of rheo-optical studies. For the case of polymer melts or concentrated solutions, the birefringence is proportional to the stress[1]. This empirical rule is summarized as the stress–optical rule (SOR). For the case of tensile deformation, the rule can be written as follows.

$$\Delta n(t) = C\sigma(t) \tag{1}$$

where $\Delta n(t)$ and $\sigma(t)$ are the birefringence and the tensile stress, respectively. The coefficient of proportionality, C, is called the stress–optical coefficient. From a theoretical point of view, the SOR indicates that the molecular origin of the stress as well as the birefringence is the orientation of flexible chains[2,3].

However, the SOR is not valid in some cases. Firstly, the SOR is invalid for fast deformations and/or at low temperatures corresponding to the glass-to-rubber transition and the glassy zones. Under these conditions, the stress includes an extra contribution similar to that of glassy materials with low molar masses[4–6]. For the stretching of films at constant speed, the stress–birefringence relationship deviates from the SOR line as represented by curve A in *Figure 1*[7,8]. The glassy stress is large at short times since it relaxes in a short time, while the stress due to the chain orientation keeps on increasing for some time. The yield phenomenon in the stretching process can be accounted for by the very fast relaxation of glassy stress, which is the major component of stress at the early stages of deformation.

Secondly, if the chain is highly orientated at relatively high temperatures, the stress and the birefringence originating from the chain orientation do not support the SOR of equation (1)[9]. In this case, the stress grows more rapidly than is expected from the SOR as shown by curve B of *Figure 1*; the stress–optical coefficient decreases with increasing stress. The relationship can still be written with a simple equation like equation (1), but with a coefficient that decreases with the stress. The deviation from equation (1) starts at the stress level corresponding to the highest modulus supported by the chain orientation, and this observation suggests that the deviation from the SOR is due to the finite extensibility of the chain[10].

Another type of deviation from the SOR is found when the system crystallizes. A well-known example is the large deformation of natural rubber, which is given in polymer textbooks[2]. In the small stress region the birefringence is porportional to the stress, but with increasing strain the birefringence starts to increase much faster than the stress and the stress–optical relationship deviates from the SOR, as shown by curve C of *Figure 1*.

In a similar fashion, if an amorphous sample (quenched from the melt) of a crystallizable polymer is stretched, strain-induced crystallization will occur and hence the simple SOR relationship will become invalid. Stein proposed a method to estimate the degree of strain-induced crystallization of rubbery materials assuming that the birefringence is a simple sum of the contribution from the crystal and from oriented chains in the amorphous portion[11]. Our interest here is to study how the stress–birefringence relationship is modified when strain-induced crystallization occurs at relatively low temperatures, *i.e.* not very much above the glass transition temperature, and to see whether the relationship can be understood using the concepts as represented by curves A–C of *Figure 1*. For this purpose, we examine the stress–birefringence relationship for

* To whom correspondence should be addressed

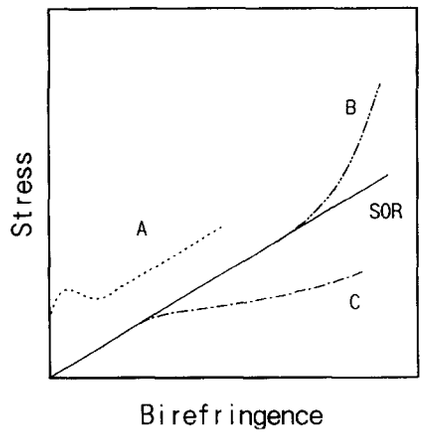

Figure 1 Illustration of the stress–birefringence relationship for the stretching process. SOR, stress–optical rule; A, deviation from the SOR near T_g; B, deviation due to high elongation of the chain; C, deviation due to crystallization

originally amorphous and non-oriented films of poly(ethylene terephthlate) (PET) during stretch at constant speed.

The strain-induced crystallization of PET films has long been studied. We do not refer to all the morphological studies since the subject is not of present interest to us. We only note that the crystalline textures obtained by strain-induced crystallization have a common feature: the crystallites are oriented in a certain direction, in contrast to the crystallites obtained by the isothermal crystallization of isotropic samples.

Salem studied the stress–strain relationship during the drawing of PET at 90°C and concluded that two regions are observed in the crystallization process; a low stress regime (regime 1) in which the stress increases slowly with the draw ratio and the crystallinity increases relatively fast; and a high stress regime (regime 2) in which the stress increases rapidly and the crystallinity increases slowly[12]. A decreasing strain rate shifts the onset of crystallization to higher draw ratios and reduces the rate at which the crystallinity increases with the draw ratio. This is because reducing the strain rate increases the time available for orientational relaxation and, therefore, increases the draw ratio required to attain the critical orientation for crystallization. The onset of regime 2 occurs at a characteristic level of crystallinity which is independent of strain rate. Salem believes that regime 1 involves the formation of a crystalline network which, at a characteristic crystallinity level, becomes sufficiently effective to sharply increase the stress generated during drawing.

The results of Salem will be helpful in understanding our stress–birefringence relationship for the process of strain-induced crystallization. On the other hand, he assigned various stages of strain-induced crystallization to certain specific features of the Mooney–Rivlin plot of the stress–strain relationship. This method may not be very adequate when the relaxation effect is important, as in the case of high temperatures or low rates of deformation. It may not be good enough at low temperatures where the stress is affected by the glassy contribution. We hope that the birefringence data in addition to the stress will give a deep insight into strain-induced crystallization.

The present paper is organized as follows. We examine the stress–birefringence relationship for amorphous PET films during uniaxial stretching at temperatures just above the glass transition temperature where the rate of spontaneous crystallization is low. We examine and try to identify various types of deviations from the simple SOR observed in the process of strain-induced crystallization. We show that one type of deviation is indeed due to strain-induced crystallization by measuring the d.s.c. of films quenched at various draw ratios. It will be revealed that the stress–birefringence relationship offers a useful *in situ* method for the easy and inexpensive determination of strain-induced crystallization.

EXPERIMENTAL

Sample

An amorphous PET film 0.3 mm thick was supplied by the Teijin Company, Ltd. The supplier's molar mass was 20000. The birefringence of the virgin film was not detectable.

Measurements of viscoelasticity and birefringence

The tensile stress and the birefringence in uniaxial elongation were measured at various temperatures from 80 to 95°C with a tensile tester equipped with a simple optical system, the details of which were described previously[13,14]. The rate of crystallization of unstretched films was quite low and not detectable within the time-scale of the experiments, about 2×10^4 s, over this temperature range.

The tensile stress, σ, and the birefringence Δn were measured simultaneously in an elongation at a constant cross-head speed corresponding to the initial elongation rate, $\dot{\epsilon}_0$, of 0.0025–0.25 s^{-1}. Since the elongation ratio, $\lambda = 1 + \dot{\epsilon}_0 t$, was large (up to about 4 for each measurement), the elongation rate was not constant during the experiment. The elongation rate at time t is given by

$$\dot{\epsilon}(t) = \dot{\epsilon}_0/\lambda(t) \tag{2}$$

In evaluating the stress and birefringence from directly detected quantities, *i.e.* the tensile force and the retardation, respectively, one needs to know the exact thickness of the specimen. We estimated the thickness assuming that the material was incompressible or that the Poisson ratio was equal to 0.5. The Poisson ratio for glassy polystyrene is reported to be 0.33[15]. We expect that the Poisson ratio at temperatures higher than the glass transition temperature is larger than 0.33, and hence the error due to the assumption of incompressibility is not too serious. The error for the birefringence is smaller than that for the stress.

Thermal analysis

The d.s.c. measurements were performed using the thermal analysis system 2000 with a DSC 2910 (TA Instrument), employing a heating rate of 10 K min^{-1}.

RESULTS AND DISCUSSION

Stress and birefringence at various cross-head speeds

Figure 2 shows the stress, σ, and the birefringence, Δn, at various draw ratios, λ, during elongation at three initial elongation rates: $\dot{\epsilon}_0 = 0.0025\ s^{-1}$, $0.025\ s^{-1}$, and $0.25\ s^{-1}$ at 85°C. At the lowest elongation speed, $\dot{\epsilon}_0 = 0.0025\ s^{-1}$, the stress increased monotonically with increasing λ and seemed to level off at high draw ratios. On the other hand, the birefringence showed a tendency to level off at first but then began to increase rapidly again at high elongation ratios. At $\dot{\epsilon}_0 = 0.025\ s^{-1}$, the stress increased gradually at

low draw ratios but rose suddenly at $\lambda = 3$. The results for the highest speed, $\dot{\epsilon}_0 = 0.25\ s^{-1}$, were similar to those for $\dot{\epsilon}_0 = 0.025\ s^{-1}$ except that σ increased sharply at very low λ and that the rate of increase of Δn decreased at high λ. Such a behaviour of σ at the early stage of elongation at high speed was commonly observed for amorphous polymers such as polystyrene and polycarbonate near the glass transition temperature[7,8].

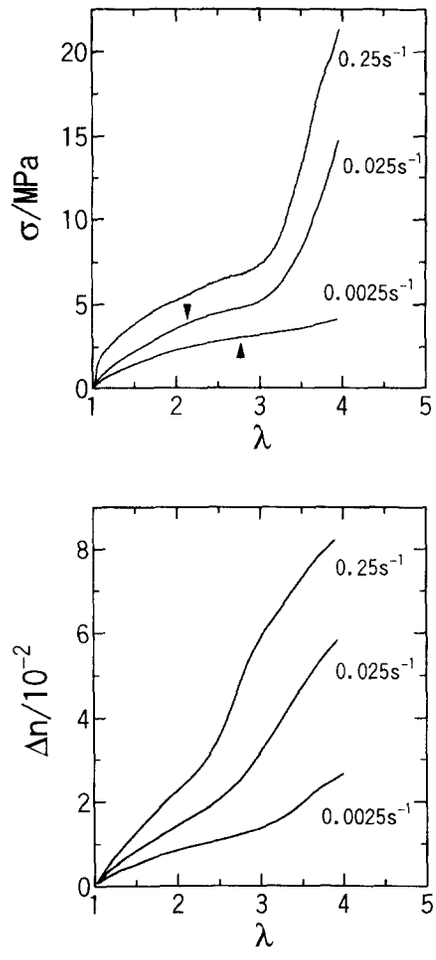

Figure 2 The stress, σ, and birefringence, Δn, plotted *versus* the draw ratio, λ, at various speeds of stretch at 85°C. Initial rates of elongation, $\dot{\epsilon}_0$, are shown in the figure

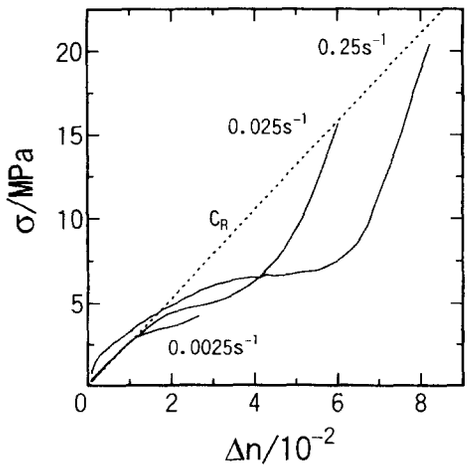

Figure 3 The stress–birefringence relationship for the data of *Figure 2*. The dashed line represents the SOR with $C = 3.80 \times 10^{-9}\ Pa^{-1}$

Stress–birefringence relationship at various cross-head speeds

Figure 3 shows the stress–birefringence relationship, hereafter called the S–B curve, for the data of *Figure 2*. The dotted line represents the SOR, equation (1), with $C = 3.80 \times 10^{-9}\ Pa^{-1}$, determined by performing dynamic mechanical and creep measurements[16].

The S–B curve for the lowest rate, $\dot{\epsilon}_0 = 0.0025\ s^{-1}$, is composed of two parts. One part is in accordance with the SOR at the initial stage of elongation, and the other deviates from the SOR line in the direction of curve C in *Figure 1*. At $\dot{\epsilon}_0 = 0.025\ s^{-1}$, the S–B curve is composed of three parts. The two at low draw ratios are the same as those at $\dot{\epsilon}_0 = 0.0025\ s^{-1}$. At high draw ratios the S–B curve rises sharply, exhibiting some similarity to curve B of *Figure 1*. The curve for the highest speed, $\dot{\epsilon}_0 = 0.25\ s^{-1}$, may seem similar to that for $\dot{\epsilon}_0 = 0.025\ s^{-1}$ but it lacks the portion that is in accordance with the SOR at low draw ratios.

The validity of the SOR at relatively low speed and in the small strain region indicates that the stress and the birefringence originate from the chain orientation in the amorphous state. Thus the system behaves like ordinary polymer melts in the small strain region. The deviation from the SOR at high speed and very low draw ratio is similar to the deviation of curve A in *Figure 1*, and is obviously related to the rapid increase of stress at the beginning of the stretch, as seen in *Figure 2*. Since the same behaviour has been observed for other amorphous polymers, the deviation from the SOR here may be attributed to the contribution of the glassy nature of the polymer to the stress. The sharp rise of the S–B curve at high draw ratios is related to the similar rise in the stress in *Figure 2* and evidently corresponds to the regime 2 of highly stretched polymer chains after a considerable degree of crystallization as observed by Salem[12].

Our main concern now is to detect the beginning of strain-induced crystallization from the S–B curve. We can tentatively take the point at which the curve first deviates from the SOR line. This was determined for the two lower speeds, $\dot{\epsilon}_0 = 0.0025\ s^{-1}$ and $0.025\ s^{-1}$, and is indicated by arrows in *Figure 2*. The point cannot be determined for the highest speed since the S–B curve does not include a portion that is in accordance with the SOR.

One can see that the strain dependence of the stress and birefringence does not change drastically at the points marked by the arrows in *Figure 2*. Thus, the onset of crystallization cannot be easily detected if the stress or the birefringence are examined separately. Salem proposed a method of detecting crystallization by applying the Mooney–Rivlin plot to the stress data[12]. However, the relaxation effect is strong above the glass transition temperature, and therefore the applicability of the Mooney–Rivlin plot, originally proposed for cross-linked networks, is questionable. In fact, the points indicated by the arrows did not correspond to any specific points, such as breaks or inflection points in the curves, in the Mooney–Rivlin plots for the stress shown in *Figure 2*. On the other hand, the combination of mechanical and optical methods in the S–B curve clearly provides some indication of the onset of strain-induced crystallization.

The stress–birefringence relationship in the stress relaxation process

After stretching the film at 85°C and $\dot{\epsilon}_0 = 0.025\ s^{-1}$ up to a certain draw, we held the length constant at the same temperature; the stress and birefringence were measured in

the stress relaxation process. The S–B relationship for stretching is represented by a dashed curve and those for relaxation by symbols in *Figure 4*.

When the length is held constant in the low λ range where the SOR holds, the S–B relationship for the relaxation process follows the SOR, so that the stress decreases along a straight line. When the relaxation is started just above the point at which the deviation from the SOR is detected, the birefringence first decreases but eventually changes to increase with time. Thus the deviation point represents the start of strain-induced crystallization at this temperature. At high draw ratios, the birefringence increases over all the stress relaxation process. The symbols at the bottom represent the Δn values after about 10^4 s of relaxation. The values may include some contribution from the crystallization after the stress has completely relaxed.

Thermal analysis

After elongation to a certain elongation ratio at $T = 85°C$ with $\dot{\epsilon}_0 = 0.025\ s^{-1}$, the sample was quickly cooled to room temperature, and d.s.c. measurements were then performed. The results are represented by solid curves in *Figure 5*. The peaks around 256°C correspond to the melting points. The peak area, and thus the quantity of crystal melting, increases with the draw ratio. The amount of increase is marked at draw ratios higher than about 2. At least a part of the increase is due to crystallization in the stretching process, as seen below. A change in the d.s.c. curve for low draw ratio samples at around 75°C corresponds to the glass transition.

For the unstretched sample, $\lambda = 1$, a crystallization peak is clearly observed at 127°C. The peak moves slightly to lower temperatures with increasing draw ratio, but the area of the peak does not vary so much below $\lambda = 2.0$. The crystallization peaks for the samples with λ higher than 2.25 display different features: the peaks are wider than for $\lambda = 1$, and the area of each peak is lower and decreases notably with increasing draw ratio. The peaks shift to lower temperatures with increasing λ. The arrow in *Figure 5* indicates the range of λ where the features of the crystallization peaks change. It may be noted that an arrow in *Figure 2* corrresponds to the same draw ratio.

The crystallization peaks for low draw ratios, $\lambda \leq 2$, are very similar to those for $\lambda = 1$, which represents crystallization in an unstretched sample. The slight orientation of the chains probably accelerates the crystallization so that the peaks shift to lower temperatures with increasing λ. The difference in the peak areas would imply that the samples with higher draw ratios, $\lambda \geq 2.25$, contain a considerable amount of crystals formed in the stretching process. Actually, the difference in the peak areas for the melting and crystallization is very small for $\lambda \leq 2$. The difference increases with λ for $\lambda \geq 2.25$. Thus the deviation from the SOR line in the S–B curve implies the start of strain-induced crystallization. Evidently, the amount of strain-induced crystallization increases with λ.

The dashed curves represent the results for films after stress relaxation for about 10^4 s at the same temperature

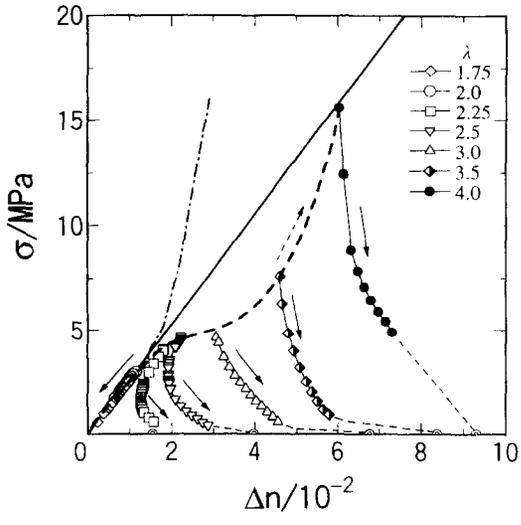

Figure 4 The stress–birefringence relationship in the stress relaxation process from various stages of stretch at 85°C with $\dot{\epsilon}_0 = 0.025\ s^{-1}$. The dashed curve represents the stretching process. The dash–dotted curve represents the S–B relationship for the chain orientation of amorphous PET derived from polycarbonate data

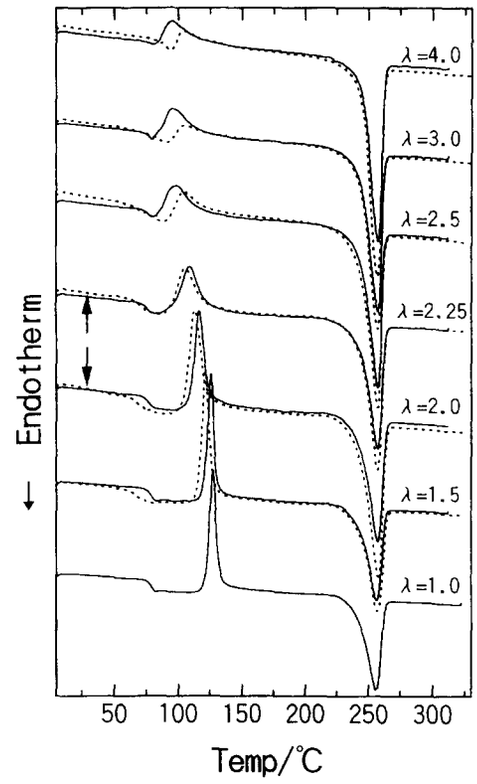

Figure 5 D.s.c. curves for quenched samples at various stages of stretch at 85°C with $\dot{\epsilon}_0 = 0.025\ s^{-1}$ (solid curves) and for samples after stress relaxation (dashed curves)

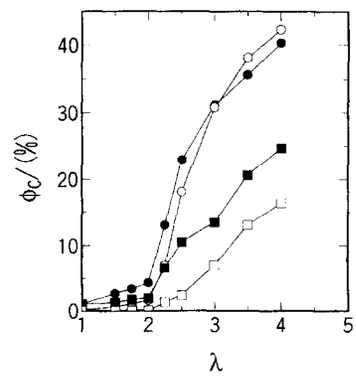

Figure 6 The degree of crystallization estimated by d.s.c. (filled symbols) and birefringence (empty symbols) for films quenched in the process of stretch (squares) and after stress relaxation (circles)

followed by rapid cooling to room temperature. The birefringence increased during the stress relaxation process, as seen in *Figure 4*. The d.s.c. curves also indicate enhanced crystallinity in the stress relaxation process.

The degree of crystallization, ϕ_c, was evaluated according to the following formula, and is shown in *Figure 6* by the filled symbols.

$$\phi_c = \frac{\Delta H_m - \Delta H_c}{\Delta H_0} \tag{3}$$

where ΔH_m and $-\Delta H_c$ are the enthalpies of melting and crystallization, respectively, estimated from the d.s.c. curve. As the heat of fusion of fully crystallized PET[17], ΔH_0, we used 117.6 J g^{-1}. The crystallinity increases rapidly with draw ratio at $\lambda > 2$, and it also increases in the stress relaxation process.

Estimation of crystallinity from birefringence

Stein estimated the amount of strain-induced crystallization of rubbery polymers according to the following equation[11]

$$\Delta n = \phi_c f \Delta n_c + (1 - \phi_c) C\sigma \tag{4}$$

where ϕ_c is the volume fraction of the crystal, f is the orientation function of the crystal, and Δn_c is the intrinsic birefringence of the crystal. The quanity $C\sigma$ represents the birefringence of the amorphous polymer as represented by the straight line in *Figure 4*. Accordingly, the highest point in the figure corresponding to $\lambda = 4$ gives a ϕ_c value very close to 0, contradicting the results of the d.s.c. measurements. This contradiction evidently originates from the upturn of the stress–birefringence curve at high stress due to the finite extensibility of the polymer chains. We need to use a stress-dependent stress–optical coefficient that takes this effect into account.

The stress-dependent stress–optical coefficient, $C(\sigma)$, cannot be obtained by direct measurements on the PET films because strain-induced crystallization is unavoidable at high draw ratios. Instead, we guessed it from polycarbonate data[9,16] as follows. Preliminary results show that a reduced stress, σ/E_R, is approximately a universal function of a reduced birefringence, $\Delta n/E_R C$, over a wide range of stress for glassy polymers[10]. Here $E_R = nkT$ is the modulus due to the segment orientation, where n is the number of Kuhn segments per unit volume. For polycarbonate[9,16], $E_R = 27$ MPa and $C = 6.0 \times 10^{-9}$ Pa^{-1} and for PET[16], $E_R = 26$ MPa and $C = 3.8 \times 10^{-9}$ Pa^{-1}. The derived relationship between Δn and σ for the orientation of chains in amorphous PET is represented by a dash–dotted curve in *Figure 4*. This curve will replace the SOR line for representing the stress–birefringence relationship for an amorphous polymer and gives

$$C(\sigma)/10^{-9}\ \mathrm{Pa}^{-1} = 3.80 + 0.0317\sigma/\mathrm{MPa} - 0.0257(\sigma/\mathrm{MPa})^2 + 0.001(\sigma/\mathrm{MPa})^3 \tag{5}$$

The values of ϕ_c estimated from the birefringence assuming $f = 1$ and $\Delta n_c = 0.22$[18,19] are shown in *Figure 6* by the empty symbols. For the films quenched in the process of stretching (squares), equation (5) was used as the C value. For those after stress relaxation (circles), the contribution from the amorphous portion is set at zero and Δn is equated with $\phi_c \Delta n_c$.

The comparison with the d.s.c. results is summarized as follows. The ϕ_c values from the birefringence are much lower than those from d.s.c. for the films quenched in the stretching process. On the other hand, the ϕ_c values having the two origins are in fairly good agreement with each other for the films after stress relaxation, at least when ϕ_c is not very low. The results seem to imply that the orientation function, f, is approximately 1 for crystals formed in the stress relaxation process, while it is much smaller for crystals formed in the stretching process.

We estimated the f values in the stretching process by assuming that the ϕ_c values from d.s.c. are the real volume fractions of the crystal; we solve equation (4) for f using the ϕ_c values from d.s.c. and the $C(\sigma)$ of equation (5). The result is shown in *Figure 7*. The curves represent theoretical values of f[20]. The upper curve is for a quasi-affine orientation, corresponding to the orientation of a rod-like body tightly embedded in an elastic material. The lower curve represents the orientation of polymer segments in a cross-linked or entangled rubbery polymer.

$$f = \frac{1}{5n_N}(\lambda^2 - \lambda^{-1}) + \frac{1}{150n_N^2}(\lambda^4 + 2\lambda - 8\lambda^{-2}) + \frac{1}{350n_N^3}(10\lambda^6 + 6\lambda^3 - 16\lambda^{-3}) \tag{6}$$

where $n_N = E_R/E_N$ is the number of segments in a chain connecting cross-link or entanglement points, and E_N is the entanglement Young's modulus and E_R is the modulus due to the segment orientation, with the values 6 MPa and 26 MPa for PET, respectively[16]. In deriving this equation, the cross-link point or the entanglement point is assumed to move according to the affine transformation and the segments are allowed to move under this restriction.

The data points at low draw ratios, $\lambda < 2.5$, are below the lower curve. The points seem to approach the upper curve at high λ. This indicates that the orientation of the strain-induced crystals is even lower than the segmental orientation in an entangled polymer at low draw ratios. The strain may slightly accelerate the crystallization but does not lead to well-oriented crystals. On the other hand, the orientation is well-approximated by the quasi-affine orientation at high draw ratios. In other words, the degree of strain-induced crystallization at high elongation can be estimated approximately from the birefringence with the use of the quasi-affine orientation function and the stress-dependent stress–optical coefficient, equation (5).

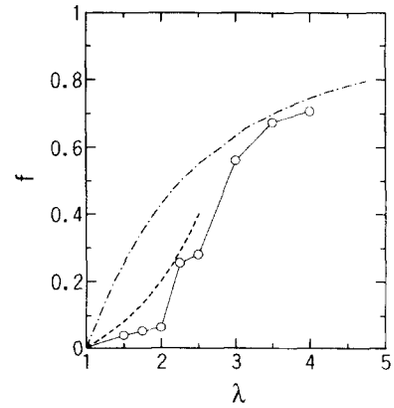

Figure 7 The orientation function, f, estimated from a comparison of the d.s.c. and birefringence measurements. Upper curve, values for quasi-affine orientation; lower curve, values for segment orientation in an entangled polymer

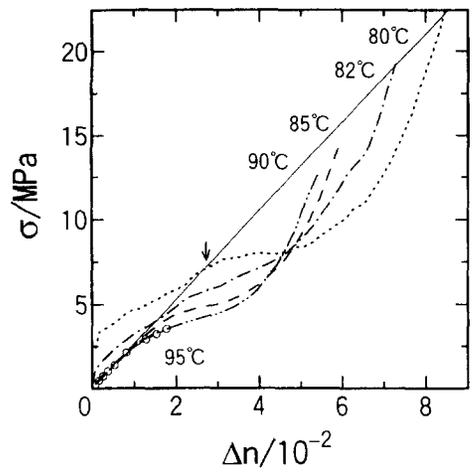

Figure 8 The stress–birefringence relationship in the stretching process at various temperatures with $\dot{\epsilon}_0 = 0.025\ s^{-1}$. The 95°C results are represented by circles

Stress–optical relationship at various temperatures

Figure 8 shows the S–B curves during elongation with an initial elongation rate, $\dot{\epsilon}_0 = 0.025\ s^{-1}$, at various temperatures between 80 and 95°C. By comparing the figure with *Figure 3*, one may say that the higher temperature corresponds to the lower stretch speed.

Some comments may be made with regard to the results at low temperatures, 80 and 82°C. In these cases the contribution of the glassy stress brings the S–B curve above the SOR line at low draw ratios. The deviation decreases rapidly with increasing λ, as expected. One may note that the curve becomes wavy when it crosses the SOR line; the curve seems to lie along the line over a certain narrow range. This result may imply that at very low temperatures there is a range when the glassy stress has relaxed out and the crystallization has not begun. If this is the case, the onset of strain-induced crystallization may be determined as the point at which the S–B curve deviates from the SOR line, denoted with an arrow for 80°C in *Figure 8*. The details relating to this point are under investigation with use of a constant rate instead of a constant speed of stretching.

CONCLUSION

The stress–birefringence relationship during uniaxial stretching may be a useful tool for detecting the strain-induced crystallization of polymer films. The start of crystallization is detected by the first deviation of the stress–birefringence curve from the line representing the stress–optical rule. Although morphological proof for the crystals was not provided, d.s.c. studies revealed that films of higher draw ratios included a certain amount of crystal, and that the crystal is different in nature from that formed in an undeformed film. At lower temperatures, the glassy component of the stress adds some complication to the stress–birefringence curve. However, the strain-induced crystallization point may still be determined provided that the crystallization starts at relatively high draw ratios, which is the case at low temperatures. We note that the present method of studying strain-induced crystallization is based on *in situ* measurements and that it is a simple and inexpensive technique.

ACKNOWLEDGEMENTS

The PET film was kindly supplied by the Teijin Company, Ltd. This study was partially supported by a Grant-in-Aid for Scientific Research (no. 09450361) from the Ministry of Education, Science, and Culture of Japan.

REFERENCES

1. Janeschitz-Kriegl, H., *Polymer Melt Rheology and Flow Birefringence*, Springer-Verlag, Berlin, 1983.
2. Treloar, L. R. G., *The Physics of Rubber Elasticity*, Clarendon, Oxford, 1958.
3. Doi, M. and Edwards, S. F., *The Theory of Polymer Dynamics*, Clarendon, Oxford, 1986.
4. Inoue, T., Okamoto, H. and Osaki, K., *Macromolecules*, 1991, **24**, 5670.
5. Inoue, T. and Osaki, K., *Macromolecules*, 1996, **29**, 1595.
6. Osaki, K., Okamoto, H., Inoue, T. and Hwang, E. -J., *Macromolecules*, 1995, **28**, 3625.
7. Okamoto, H., Inoue, T. and Osaki, K., *Macromolecules*, 1992, **25**, 3413.
8. Inoue, T., Okamoto, H. and Osaki, K., *Macromolecules*, 1992, **25**, 7069.
9. Kroeger, M., Laup, C. and Muller, R., *Macromolecules*, 1997, **30**, 526.
10. Inoue, T. and Osaki, K., submitted for publication.
11. Stein, H., *Polym. Eng. Sci.*, 1976, **16**, 152.
12. Salem, D. R., *Polymer*, 1992, **33**, 3182.
13. Kimura, S., Osaki, K. and Kurata, M., *J. Polym. Sci. Polym. Phys. Ed.*, 1981, **19**, 151.
14. Inoue, T., Hayashihara, H., Okamoto, H. and Osaki, K., *J. Polym. Sci. Polym. Phys. Ed.*, 1992, **30**, 409.
15. Wood, L. A., in *Polymer Handbook*, 3rd edn, ed. J. Brandrup and E. H. Immergut, Wiley, New York, 1989, p. V-83.
16. Ryu, D. S., Inoue, T. and Osaki, K., submitted for publication.
17. Starkweather, H. W., Zoller, P. and Jones, G. A., *J. Polym. Sci. Polym. Phys. Ed.*, 1983, **21**, 295.
18. Dumbleton, J. H., *J. Polym. Sci., Part A-2*, 1968, **6**, 795.
19. De Vries, A. J., Bonnebat, C. and Beatemps, J., *J. Polym. Sci. Polym. Symp.*, 1977, **58**, 109.
20. Rietsch, F., Duckett, R. A. and Ward, I. M., *Polymer*, 1979, **20**, 1133.